



IMPLEMENTATION OF A SECOND-ORDER INTERPOLATION SCHEME FOR THE CONVECTIVE TERMS OF A SEMI-IMPLICIT TWO-PHASE FLOW ANALYSIS SOLVER

H.K. Cho,^{*1} H.D. Lee,² I.K. Park³ and J.J. Jeong³

물-기체 2상 유동 해석을 위한 Semi-Implicit 방법의 대류항에 대한 이차정확도 확장

조형규,^{*1} 이희동,² 박익규,³ 정재준³

가압 경수로의 주요 기기에서 발생할 수 있는 과도 2상 유동 (Two-phase flow) 현상에 대한 해석을 수행하기 위해 원자로 기기 열수력 해석 코드를 개발 중에 있다. 개발 중인 기기 열수력 해석 코드는 지배 방정식으로 Two-phase, three-field model을 사용하고 있으며, 복잡한 기하학적 형상의 원자로 기기를 모사하기 위해 비정렬 격자계 (Unstructured grid)를 활용하고 있다. 수치해석 기법으로는, 원자로 계통 해석코드 RELAP5가 사용 중이며 대부분의 원자로 내 2상 유동 조건에서 안정적이며 정확하다고 알려진 Semi-implicit 방법을 적용하였다. 그러나 기존의 Semi-implicit 방법은 1차원, 엇갈림격자 (Staggered grid)에 대해 개발되었기 때문에, 이를 다차원, 비정렬, 비엇갈림 격자 (Non-staggered grid)에 적용하기 위해 기존의 Semi-implicit 방법을 수정하였다. 본 논문에서는 Semi-implicit 방법의 대류항을 이차정확도를 갖도록 확장하였으며, 이차정확도에 의한 수치확산의 감소를 평가하기 위해 수행된 수치시험의 결과를 기술하였다. 이차정확도 및 일차정확도로 계산된 값을 해석해 또는 격자 수렴성 시험을 통해 평가해 본 결과, 이차정확도 계산 시 수치 확산의 감소 확인하였다.

A two-phase (gas and liquid) flow analysis solver, named CUPID, has been developed for a realistic simulation of transient two-phase flows in light water nuclear reactor components. In the CUPID solver, a two-fluid three-field model is adopted and the governing equations are solved on unstructured grids for flow analyses in complicated geometries. For the numerical solution scheme, the semi-implicit method of the RELAP5 code, which has been proved to be very stable and accurate for most practical applications of nuclear thermal hydraulics, was used with some modifications for an application to unstructured non-staggered grids. This paper is concerned with the effects of interpolation schemes on the simulation of two-phase flows. In order to stabilize a numerical solution and assure a high numerical accuracy, the second-order upwind scheme is implemented into the CUPID code in the present paper. Some numerical tests have been performed with the implemented scheme and the comparison results between the second-order and first-order upwind schemes are introduced in the present paper. The comparison results among the two interpolation schemes and either the exact solutions or the mesh convergence studies showed the reduced numerical diffusion with the second order scheme.

Key Words : 2상 유동 (Two-Phase Flow), 반내재적 기법 (Semi-Implicit Method), 원자로 열수력 (Nuclear Thermal Hydraulics)

Nomenclature

1 한국원자력연구원

2 학생회원, KAIST

3 정회원, 한국원자력연구원

* Corresponding author, E-mail: hkcho@kaeri.re.kr

c_p	Specific heat
dx	Distance vector
e	Internal energy
E	Energy diffusion term



F	Interfacial drag force term
g	Gravity acceleration
h	Enthalpy
H	Interfacial heat transfer coefficient
j	Superficial velocity
k	Conductivity
M	Interfacial momentum transfer term
\dot{m}	Mass flow rate
N_f	Number of faces in a cell
n_p	Number of nodes on a face
P	Pressure
Q	Interfacial heat transfer term
q	Wall heat transfer term
q''	Wall heat flux
S	Entrainment or De-entrainment rate
t	Time
T	Temperature
u	Velocity
V	Volume
W	Width
X	Non-condensable quality

Greek Letter

α	Volume fraction
\mathcal{X}	Interface drag factor
Γ	Vapor generation rate
η	Fraction of vapor generated from droplets
Φ	Slope limiter
θ	Convective quantity
ρ	Density
τ	Shear stress
Ψ	Volume flow
Ω	Total mass transfer rate

Subscripts

d	Droplet
DE	De-entrainment
E	Entrainment
g	Gas
i	Interface
in	Inlet
k	= g, l or d

l	Liquid
m	Mixture
\bar{m}	Mean
n	Non-condensable
n	Node
sat	Saturation
v	Vapor
w	Wall
$wall$	Wall

1. INTRODUCTION

The need for a multi-dimensional analysis for the thermal hydraulic phenomena in a component of a nuclear reactor is increasing with the advanced designs of a reactor and a safety system. In the case of APR1400, Korean advanced power reactor, multi-dimensional phenomena inside the reactor vessel during a postulated loss of coolant accident has become major technical issues for consideration [1]. These include the ECC bypass of a DVI (Direct Vessel Injection) system and a downcomer boiling during the reflood phase of a LBLOCA. These phenomena are characterized by the combination of a boiling due to a downcomer wall heat transfer, multi-dimensional counter-current flow, lateral motion of bubbles and droplets, flow regime change, bulk condensation, phase separation, etc. The resolution of these issues was addressed through experiments, and not by state-of-the-art system codes or CFD codes. Motivated by these issues, the development of a numerical solver for a component analysis code, named CUPID, is in progress at Korea Atomic Energy Research Institute (KAERI). The objective of the development is to support a resolution of the thermal hydraulic issues regarding the transient multi-dimensional two-phase flow phenomena which can arise in a component of an advanced reactor.

The important features of the CUPID code are listed below.

- Governing equations: three-dimensional, two-fluid, three-field model
- Transient flows
- Laminar and turbulent flows
- Porous media and open media
- Turbulence models: algebraic model and standard k- ϵ Model
- Fluid solver algorithms: semi-implicit, SMAC and SIMPLE

- Unstructured mesh

In our previous papers [2,3,4], the numerical schemes for the two-fluid model were described and various conceptual problems have been solved for the verification of the solvers. The first-order upwind interpolation scheme, however, had been employed for our previous numerical tests. In order to reduce the numerical diffusion associated with the first-order upwind scheme, a second-order upwind scheme for two-phase flows is introduced. The present paper describes the second-order scheme and the suppressed numerical diffusion of the calculation results.

2. GOVERNING EQUATIONS OF THE TWO-FLUID MODEL

The present numerical solver needs to have an applicability to both porous medium and open medium to simulate the multi-dimensional two phase flow behavior in a reactor component. Basically, the present numerical solver adopted the two-fluid three-field model for two-phase flows. But for the open medium, the solver adopts the two-field model rather than the three-field model since it is hard to define the entrainment rate and deposition rate in open medium. The three-field model can be changed to a two-field model easily by fixing the values of the entrainment rate and the deposition rate to zero.

In the two-fluid three-field model, the mass, energy, and momentum equations for each field are established separately and, then, they are linked by the interfacial mass, energy, and momentum transfer models.

The continuity equation for k-field is

$$\frac{\partial}{\partial t}(\alpha_k \rho_k) + \nabla \cdot (\alpha_k \rho_k \underline{u}_k) = \Omega_k, \quad (1)$$

where,

$$\Omega_g = \Gamma_v + \Gamma_{wall}, \quad (2)$$

$$\Omega_l = -(1-\eta)\Gamma_v - \Gamma_{wall} - S_E + S_{DE}, \quad (3)$$

$$\Omega_d = -\eta\Gamma_v + S_E - S_{DE}, \quad (4)$$

The non-condensable gases when present are contained in the vapor field, and these are assumed to move with

the same velocity and have the same temperature as the vapor phase. Thus, the continuity equation for the total non-condensable component is given as

$$\frac{\partial}{\partial t}(\alpha_g \rho_g X_n) + \nabla \cdot (\alpha_g \rho_g X_n \underline{u}_g) = 0, \quad (5)$$

where the non-condensable quality X_n is defined as the ratio of the non-condensable gas mass to the total gaseous phase mass.

The momentum equation for the k-field is

$$\begin{aligned} \frac{\partial}{\partial t}(\alpha_k \rho_k \underline{u}_k) + \nabla \cdot (\alpha_k \rho_k \underline{u}_k \underline{u}_k) = & -\alpha_k \nabla P \\ & + \nabla \cdot [\alpha_k (\underline{\tau}_k + \underline{\tau}_k^T)] + \alpha_k \rho_k \underline{g} + \underline{M}_{ik}, \end{aligned} \quad (6)$$

where \underline{M}_{ik} is the interfacial momentum transfer term.

In the energy equations, it is assumed that the continuous liquid and entrained liquid are in a thermal equilibrium, i.e., $T_d = T_l$. This is a good approximation for most of the applications of interest. As a result, two energy equations are used, i.e., one for the gas field and one for the combined field of the continuous and entrained liquids.

$$\begin{aligned} \frac{\partial}{\partial t}(\alpha_g \rho_g e_g) + \nabla \cdot (\alpha_g \rho_g e_g \underline{u}_g) = & -P \frac{\partial}{\partial t} \alpha_g + E_g^D \\ & - P \nabla \cdot (\alpha_g \underline{u}_g) + Q_{ig} - Q_{gl} + q_{wg}, \end{aligned} \quad (7)$$

$$\begin{aligned} \frac{\partial}{\partial t}[(1-\alpha_g)\rho_l e_l] + \nabla \cdot [(\alpha_l \underline{u}_l + \alpha_d \underline{u}_d)\rho_l e_l] = & -P \frac{\partial}{\partial t}(1-\alpha_g) \\ & + E_l^D - P \nabla \cdot (\alpha_l \underline{u}_l + \alpha_d \underline{u}_d) \\ & + Q_{il} + Q_{gl} + q_{wl}, \end{aligned} \quad (8)$$

where E_k^D includes the conduction, turbulent energy source, and viscous dissipation that are represented in terms of a diffusion.

The interfacial energy transfer terms, Q_{ig} and Q_{il} , in Eqs. (7) and (8) are modeled as

$$Q_{ig} = P_s / P \cdot H_{ig} A_i (T_{sat} - T_g) + \Gamma_v h_{gi} + \Gamma_{wall} h_{g,sat}, \quad (9)$$

$$Q_{il} = H_{il} A_i (T_{sat} - T_l) - \Gamma_v h_{li} - \Gamma_{wall} h_l, \quad (10)$$

where $(h_{gi}, h_{li}) = (h_{g,sat}, h_l)$ if $\Gamma \geq 0$,

$(h_{gi}, h_{li}) = (h_g, h_{l,sat})$ if $\Gamma < 0$.



Because the sum of Q_{ig} and Q_{il} is zero, the volumetric vapor generation rate is represented as

$$\Gamma_v = -\frac{\frac{P_s}{P} H_{ig} A_i (T_{sat} - T_g) + H_{il} A_i (T_{sat} - T_l)}{h_{gi} - h_{li}}, \quad (11)$$

The term Q_{gl} in Eqs. (7) and (8) is the sensible heat transfer rate per unit volume at the non-condensable gas-liquid interface:

$$Q_{gl} = (P - P_s) / P \cdot H_{gl} A_i (T_g - T_l), \quad (12)$$

The interfacial momentum transfer term, \underline{M}_{ik} in Eq. (6), includes the interfacial drag, the momentum exchange due to the interface and wall mass transfer and various non-drag forces such as lift force, virtual mass force etc. For simplicity, however, the non-drag forces are omitted hereinafter and, then \underline{M}_{ik} is written as:

$$\underline{M}_{ig} = -\underline{F}_{gl} - \underline{F}_{gd} + \Gamma_v \underline{u}_{gi} + \Gamma_{wall} \underline{u}_{gi}, \quad (13)$$

$$\begin{aligned} \underline{M}_{il} &= -\underline{F}_{gl} - (1 - \eta) \Gamma_v \underline{u}_{li} - \Gamma_{wall} \underline{u}_{li} \\ &- S_E \underline{u}_l + S_{DE} \underline{u}_d, \end{aligned} \quad (14)$$

$$\underline{M}_{id} = -\underline{F}_{gd} - \eta \Gamma_v \underline{u}_{di} + S_E \underline{u}_l - S_{DE} \underline{u}_d. \quad (15)$$

The interface velocities, \underline{u}_{ki} , are needed to obtain the interfacial momentum transfer due to the interface mass transfer. These are determined using a donor formulation concept.

The independent state variables P , α_k , e_k and X_n and phasic velocities \underline{u}_k are the unknowns of the present solver and the dependent variables such as the phasic density, phasic temperature, the saturation temperature, the saturation pressure are expressed as functions of the independent state variables from the equations of the states (EOS).

The present numerical solver adopted the semi-implicit numerical scheme and the detailed procedure of the numerical algorithm was reported in our previous paper by Ref. 2.

3. SECOND ORDER UPWIND METHOD FOR THE

TWO-PHASE FLOW SOLVER

In our previous studies, the first-order upwind scheme and the second-order central difference scheme for the convective terms of the governing equations had been used for the numerical tests. So as to stabilize a numerical solution and assure a high numerical accuracy, the second-order upwind scheme was implemented into the CUPID code in the present paper. The convective terms in the current numerical solver and their discretized forms are:

for a continuity equation for k-phase,

$$\int \nabla \cdot (\alpha_k \rho_k \underline{u}_k^{n+1}) dV \approx \sum_f (\alpha_k \rho_k)_f (\psi_k)_f^{n+1}, \quad (16)$$

for a continuity equation for non-condensable gas,

$$\int \nabla \cdot (\alpha_g \rho_g X_n \underline{u}_g^{n+1}) dV \approx \sum_f (\alpha_g \rho_g X_n)_f (\psi_g)_f^{n+1}, \quad (17)$$

for a energy equation for non-condensable gas,

$$\int \nabla \cdot (\alpha_k \rho_k e_k \underline{u}_k^{n+1}) dV \approx \sum_f (\alpha_k \rho_k e_k)_f (\psi_k)_f^{n+1}, \quad (18)$$

for a momentum equation for k-phase, the following non-conservative form was used.

$$\begin{aligned} &\frac{\partial}{\partial t} (\alpha_k \rho_k \underline{u}_k) + \nabla \cdot (\alpha_k \rho_k \underline{u}_k \underline{u}_k) \\ &= \alpha_k \rho_k \frac{\partial \underline{u}_k}{\partial t} + \nabla \cdot (\alpha_k \rho_k \underline{u}_k \underline{u}_k) - \underline{u}_k \nabla \cdot (\alpha_k \rho_k \underline{u}_k) \\ &- \underline{u}_k \Omega_k. \end{aligned} \quad (19)$$

Therefore, it has two convective terms:

$$\int \nabla \cdot (\alpha_k \rho_k \underline{u}_k \underline{u}_k^n) dV \approx \sum_f (\alpha_k \rho_k \underline{u}_k)_f (\psi_k)_f^n, \quad (20)$$

and

$$- \int \underline{u}_k \nabla \cdot (\alpha_k \rho_k \underline{u}_k) dV \approx -\underline{u}_k \sum_f (\alpha_k \rho_k)_f (\psi_k)_f^n, \quad (21)$$

where $(\psi_k)_f = (\underline{u}_k \cdot \underline{\mathcal{S}})_f$: volume flow rate. In general, the convective terms can be expressed by

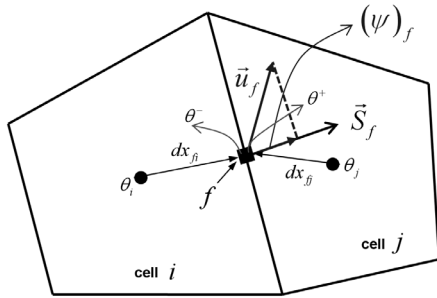


Fig. 1 Face value evaluation for upwind scheme

$$A \sum_f (\theta)_f (\psi_k)_f, \tag{22}$$

where $(\theta)_f$: convective quantity. As indicated in Fig. 1, the convective quantities $(\theta)_f$ are evaluated in the first-order upwind scheme as

$$(\theta)_f = \begin{cases} \theta^- = \theta_i & \text{if } (\psi)_f \geq 0 \\ \theta^+ = \theta_j & \text{if } (\psi)_f < 0 \end{cases} \tag{23}$$

In the case of the second-order upwind scheme, they are calculated by

$$(\theta)_f = \begin{cases} \theta^- = \theta_i + \Phi(\nabla\theta)_i \cdot \underline{dx}_{fi} & \text{if } (\psi)_f \geq 0 \\ \theta^+ = \theta_j + \Phi(\nabla\theta)_j \cdot \underline{dx}_{fj} & \text{if } (\psi)_f < 0, \end{cases} \tag{24}$$

where $\underline{dx}_{kf} = \underline{x}_f - \underline{x}_k$,

Φ : slope limiter.

In order to obtain $\nabla\theta$ at the center of a cell, Frink's restructuring method [5] was applied which is based on the Green-Gauss method.

$$(\nabla\theta)_i = \frac{1}{V} \sum_f \bar{\theta}_f \underline{S}_f, \tag{25}$$

where $\bar{\theta}_f = \sum_{k=1}^{n_p} \theta_{n,k} / n_p$: a cell face value calculated by the interpolation of the face node values, n_p : the number of nodes on the face.

The node values of a face θ_n were determined using the pseudo-Laplacian weighting method [6] as shown in Fig. 2.

In a two-phase flow, there might be a discontinuity of

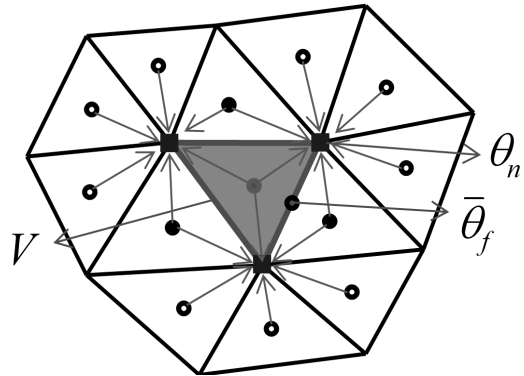


Fig. 2 Frink's Pseudo-Laplacian weighting method

convective variables between two cells, which can cause unphysical oscillatory numerical results. To suppress the oscillation and to assure the stability of the interpolation scheme, the slope limiter (Φ) proposed by Barth and Jespersen [7] was applied in the following forms,

$$\Phi = \min(\phi_1, \dots, \phi_r), \tag{26}$$

where $\Delta_{\max} = \max(\theta_j, \theta_i) - \theta_i$,

$$\Delta_{\min} = \max(\theta_j, \theta_i) - \theta_i,$$

$$\Delta_j = (\bar{\theta}_f)_j - \theta_i,$$

$$\phi_j = \begin{cases} \min(1, \Delta_{\max} / \Delta_j), & \text{if } \Delta_j > 0 \\ \min(1, \Delta_{\min} / \Delta_j), & \text{if } \Delta_j < 0 \\ 1 & \text{if } \Delta_j = 0 \end{cases}$$

4. VERIFICATION OF THE SECOND ORDER UPWIND METHOD

To evaluate the performance of the present approach, numerical tests were performed first for both single-phase and two-phase flows: a single-phase laminar flow with a constant wall heat flux and a phase separation respectively.

Fig. 3 shows the two-dimensional computational domain and boundary conditions of the single-phase laminar flow example problem. For a simplicity of the analytical solution, the fluid properties such as the viscosity, density, heat conductivity were assumed to be constants, 0.1 Ns/m², 1000 kg/m³, 3000 W/mK respectively. In this case, the analytical solution of the fully developed temperature profile is [8]

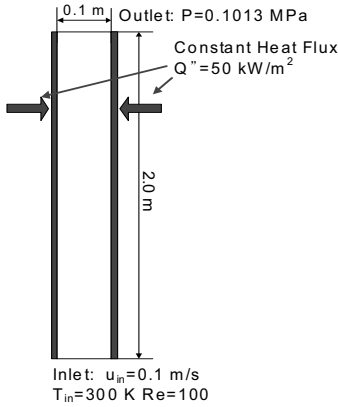


Fig. 3 Computational domain and boundary conditions of the laminar flow calculation

$$\frac{T_w - T(x)}{T_w - T_m} = \frac{35}{136} \left[5 - 6 \left(\frac{x}{0.5 \cdot W} \right)^2 + \left(\frac{x}{0.5 \cdot W} \right)^4 \right], \quad (27)$$

where $T_m(y) = T_{m,m} + \frac{2q''}{\dot{m}c_p} y$,

$$\frac{T_w - T_m}{q'' \cdot 2W / k} = \frac{17}{140}.$$

The calculations were performed with relatively coarse (5×50) and fine (10×50) meshes applying both first-order and second-order schemes to each mesh so that total four calculation cases were selected for the single-phase flow numerical test.

Fig. 4. shows the temperature comparison results between the analytical solution and the calculation results of the four cases when the flow was fully developed. The comparison results showed that the present solver can capture the exact solution and more accurate results can be obtained with the second-order scheme in the same mesh.

As the second test for the verification of the second-order scheme, a phase separation problem was simulated. Fig. 5. shows the two-dimensional computational domain and the initial conditions of the problem. Initially, the cavity was filled with a two-phase mixture of which void fraction was 0.5. As the calculation started, a phase separation was induced by a density difference so that two steep void waves traveled from the top and bottom ends simultaneously as shown in Fig. 6-(a). The two void waves met at the middle of a section, which resulted in

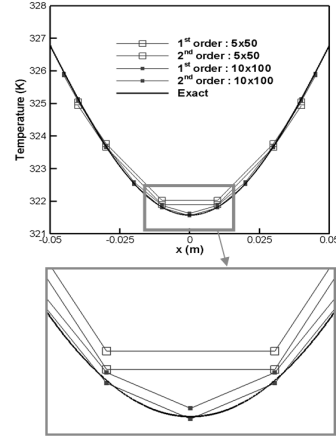


Fig. 4 Temperature distribution comparison results : exact solution vs calculation results

the formation of a sharp interface after the phase separation was complete (Fig. 6-(b)). As shown in Fig. 6, this phase separation process was predicted qualitatively well by the present solver.

Neglecting the momentum flux terms and virtual mass forces, we can obtain the analytical solutions of the void propagation velocities as below[9],

$$u_l = -\frac{\alpha_g \alpha_l (\rho_m - \rho_g) g}{\chi_l} \quad \text{and}$$

$$u_g = \frac{\alpha_g \alpha_l (\rho_m - \rho_g) g}{\chi_l}, \quad (28)$$

where $\rho_m = \alpha_l \rho_l + \alpha_g \rho_g$.

For the simplicity of the analytical solution, the following simple algebraic model of the interfacial drag model was used instead of Eq.(21) and (22).

$$\chi_i = 40000 \cdot \alpha_g \alpha_l, \quad (29)$$

As with the previous example of the laminar flow, four calculation cases were performed with the first-order and second-order schemes in relatively coarse (20×20) and fine (40×40) meshes. The numbers of meshes in this calculation are not sufficient to capture the sharp void fraction gradient along the channel elevation. But we used the coarse meshes to show the decreased numerical diffusion more apparently.

In Fig. 7, the analytical solution was compared with the

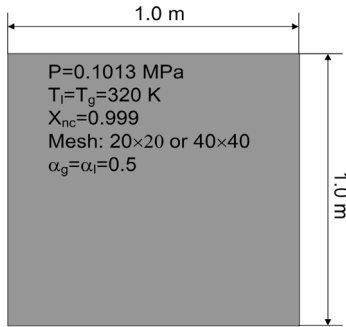
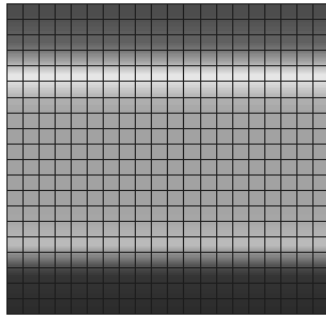
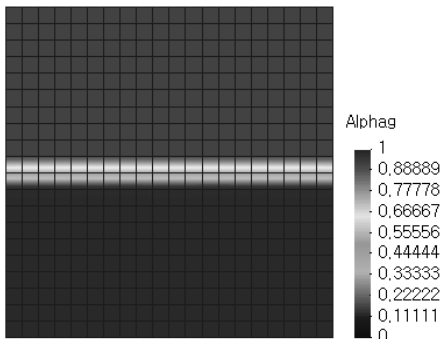


Fig. 5 Computational domain and initial conditions of the phase separation calculation



(a) $t=2.0\text{s}$



(b) $t=5.0\text{s}$

Fig. 6 Phase separation calculation results : void fraction

four calculation results. As can be seen in the comparison result, the void wave propagation was predicted well by the present solver even though the void fraction profiles were smeared due to a numerical diffusion. Moreover the comparison results showed the reduced numerical diffusion with the second order scheme as expected.

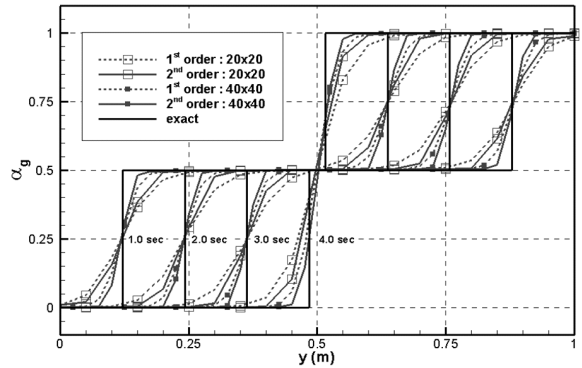


Fig. 7 Void fraction comparison results : exact solution vs calculation results

From these two examples of the calculations, it was verified that the second-order upwind interpolation scheme was implemented appropriately and the numerical diffusion can be reduced with it. Moreover, it was shown that the Barth limiter, originally proposed for a single phase compressible flow, is applicable for a two-phase flow analysis.

4. CONCLUSION

A component-scale two-phase analysis code, CUPID, has been developed for a realistic simulation of transient two-phase flows in light water nuclear reactor components. In the present paper, the recent improvements to the CUPID code were introduced, particularly, the implementation of the second-order upwind scheme for the convection terms. In order to verify the implemented features, some verification tests were performed. The numerical tests using the second-order upwind scheme indicated a reduced numerical diffusion even in a two-phase flow condition which contains a sharp interface. During the calculation for the phase separation, the unstable oscillatory behavior of a void wave was not observed, which means the applied slope limiter worked appropriately.

In the future, various validation works will be carried out against a wide range of multi-dimensional two-phase flows for the quantitative assessments of the numerical solver.

ACKNOWLEDGEMENT

This work was supported by Nuclear Research & Development Program of the KOSEF (Korea Science and



Engineering Foundation) grant funded by the MEST (Ministry of Education, Science and Technology) of the Korean government (Grant code: M20702040002 - 08M0204-00210).

REFERENCES

- [1] 2003, Song, C.-H., Baek, W.P., Chung, M.K. and Park, J.K., "Multi-Dimensional Thermal Hydraulic Phenomena in Advanced Nuclear Reactor Systems: Current Status and Perspectives of R&D Program in KAERI," *Proc. NURETH-10*, Seoul, Korea.
- [2] 2008, Jeong, J.J., Yoon, H.Y., Park, I.K., Cho, H.K. and Kim, J., "A Semi-implicit Numerical Scheme for Transient Two-phase Flows on Unstructured Grids," *Nuclear Engineering and Design*, Vol.238, pp.3403-3412.
- [3] 2009, Yoon, H.Y., Park, I.K., Lee, Y.J. and Jeong, J.J., "An Unstructured SMAC Algorithm for Thermal Non-equilibrium Two-phase Flows," *International Communications in Heat and Mass Transfer*, Vol.36, pp.16-24.
- [4] 2008, Kim, J. et al., "Unstructured-mesh Pressure-based Algorithm for the Simulation of Two-phase Flows in a Light Water Nuclear Reactor," *Proc. NUTHOS-7*, Seoul Korea.
- [5] 1991, Frink, N.T. et al., "A Fast Upwind Solver for the Euler Equations on Three-Dimensional Unstructured Meshes," *AIAA-91-0102*, Reno, Nevada.
- [6] 1994, Frink, N.T., "Recent Progress Toward a Three-dimensional Unstructured Navier-Stokes Flow Solver," *AIAA-94-0061*, Reno, Nevada.
- [7] 1989, Barth, J. and Jespersen, D.C., "The Design and Application of Upwind Schemes on Unstructured Meshes," *AIAA-89-0366*, Reno, Nevada.
- [8] 1987, Kakac, S. et al., *Handbook of Single-Phase Convective Heat Transfer (I)*, John Wiley & Sons, Inc., pp.3.30-3.32.
- [9] 2006, Staedtke, H., *Gas Dynamic Aspects of Two-phase Flow*, Wiley-VCH Verlag GmbH & Co. KGaA Weinheim, pp.143-147.